We are IntechOpen, the world's leading publisher of Open Access books Built by scientists, for scientists

6,900
Open access books available

185,000
International authors and editors

200M
Downloads

Our authors are among the

154
Countries delivered to

TOP 1%
most cited scientists

12.2%
Contributors from top 500 universities



WEB OF SCIENCE™

Selection of our books indexed in the Book Citation Index in Web of Science™ Core Collection (BKCI)

Interested in publishing with us?
Contact book.department@intechopen.com

Numbers displayed above are based on latest data collected.
For more information visit www.intechopen.com



Chapter

Power Flow Management Algorithm for a Remote Microgrid Based on Artificial Intelligence Techniques

Karim Belmokhtar and Mauricio Higuita Cano

Abstract

This paper presents a novel power flow management algorithm for remote microgrids based on artificial intelligence (AI) algorithms. The objectives of this power management system are enhancing microgrid reliability, improving renewable energy source (RES) integration, and performing active/reactive power control for remote microgrids using the fuzzy logic. This paper evaluates the performance of the proposed algorithm, which consists of both sharing diesel genset active power and regulating reactive power by using stepped and variable profiles of the load, wind speed and solar irradiation. According to the simulation results, better performance is achieved regardless of the rapid variation of different profiles. Thus, both stability and reliability of remote microgrids are demonstrated with the proposed algorithm. Indeed, the active/reactive power control algorithm responds quickly to different events on the remote microgrid, especially to rapid voltage/frequency variations on the AC-link system.

Keywords: power management system, artificial intelligence (AI), renewable energy sources (RES), remote microgrid, fuzzy logic (FL)

1. Introduction

Renewable energy sources (RES) have been positioned as an attractive solution to reduce dependence on fossil fuels while minimizing greenhouse gas emissions (GHG) [1]. RES such as wind energy and solar (PV) energy have been extensively researched in the literature [2–5]. One of the main issues with RES is that their natural intermittency can affect the stability of the microgrid. On the other hand, technical issues associated with high penetration rates of RES related to their intermittency, different dynamics and response times can be addressed by using energy storage systems (ESS) and advanced power management systems (PMS) [3].

ESS has been identified as a solution to increase energy reliability, improve the balance in energy production, and better manage load demand on the microgrid. The main purpose of ESS in the microgrid is to store excess power from an intermittent RES and return the stored energy to meet load consumption as a function of supply and demand [6]. In addition, ESS can be used in several applications in order

IntechOpen

to improve both microgrid stability and power quality. According to the literature, ESS applications include load smoothing/peak shaving, power quality improvement, increased renewable energy penetration and emergency storage systems [7–9].

Power management systems (PMS) can be divided into two categories: (i) PMS based on optimization methods and (ii) PMS based on artificial intelligence techniques [10]. Mostly, the PMS based on optimization methods involve a multi-objective function, which maximizes microgrid effectiveness, minimizes fossil fuel consumption and meets operation conditions requirements. A PMS based on optimization has recently been presented by Gao et al. [11]. In this study, optimal control is proposed using a three-level control architecture. In the third control level, a multi-objective is responsible for minimizing fuel consumption and GHGs as well as scheduling operational maintenance. The second control level is based on the discrete algorithms that regulate the frequency/voltage from active/reactive power according to the load demand. Lastly, in this study, the first control level is responsible for following the reference control between the components of the system. A multi-objective optimization in cloud platform is presented by Li et al. [12]. The optimization function is based on the particle swarm optimization (PSO) method. One of the objectives of this work is to use the cloud to perform the algorithm calculation in real time. Otherwise, hybridization between AI techniques and linear programming-based multi-objective optimization is presented in [13]. In this study, simulation results proved the effectiveness of the proposed multi-objective intelligent energy management using an FL-based expert system. A review of the advanced microgrid supervisory controllers (MGSC) and energy management systems (EMS) is presented by Meng et al. [14]. The hierarchical control, definitions and issues are presented. The centralized MGSC/EMS is usually more suitable for small-scale microgrid applications where centralized information gathering and decision-making can be performed with low communication and computing costs. Among the techniques or methods used on centralized control, a review has been presented by the authors with regard to genetic algorithms, swarm algorithms, linear and non-linear optimization, the rule-based system and machine learning systems. On the other hand, the decentralized MGSC/EMS can be more desirable when the microgrid is large or the generation, consumption and storage are widely dispersed, which makes centralized data acquisition difficult or costly. The multi-agent system (MAS) based on MGSC/EMS has become a prominent research direction, as it provides the probability to actualize decentralized management functions.

PMS based on artificial intelligence (AI) algorithms are easier to implement and are more widely used for real-time microgrid control. Furthermore, it is not necessary to know the exact mathematical model for each RES or energy storage device in the microgrid. Zahraee et al. [15] presented the applications of AI techniques for hybrid energy systems (HES). The authors present a summary of research concerning the use of AI algorithms for designing, planning and controlling problems in the fields of HES. AI algorithms are mostly used because they require less computational time, show better accuracy and better convergence in comparison to traditional methods. The research focuses on hybridization between optimization and AI techniques. These approaches have been proven to be faster, more accurate and more powerful than classical methods. Similarly, Rajesh et al. [16] presented a review of AC microgrid control. The islanded and grid-connected modes of microgrid operation are presented. The control techniques and their different hierarchy levels are identified and explained in detail. According to the review, for primary control level, droop control is used for small and large microgrids as it

provides a high degree of plug-and-play capability. Centralized or decentralized control can be used on the second control level. Centralized control is more suitable for small-scale microgrid applications and decentralized control is normally used for large-scale multi-user microgrids. The tertiary control is applied when the microgrid operates in grid-connected mode. Reactive power compensation techniques for microgrids are evaluated by [17]. An overview of the challenges and power quality issues faced by microgrids are identified. Likewise, the different compensation methods, various control techniques, algorithms and devices are investigated in this study. A multi-agent system (MAS) decentralized energy management in a microgrid is presented in [18]. The microgrid system is composed of a battery/genset/FC/PV/hydro plant and variable electrical load. This study demonstrates that hybrid MAS – fuzzy Q-Learning is appropriate to solve the complex issues of energy management in a stand-alone microgrid by controlling the power flow between RES and ESS. Likewise, a control strategy for a Flywheel Energy Storage System (FESS) using the Artificial Neural Network (ANN) is presented by Daoud et al. [19]. The FESS is connected to an electric network. The charge/discharge from the electrical grid to FESS is used as grid frequency support/control, power conditioning or uninterruptible power supply (UPS) applications. The simulation and experimental tests show good results of the ANN strategy compared with classical power control strategies. In addition to its simplicity, the ANN strategy exhibits fewer tuning problems and requires less controller effort. Mallesham et al. [20] propose an automatic first-control level of microgrid using AI techniques. The difficulty in tuning a large number of parameters in complex systems can be achieved through AI techniques. This study compared various AI techniques with traditional power control strategies. The simulation results show that optimal tuning of multiple parameters in a non-linear microgrid using BFO techniques is better than PSO, GA and classical methods.

In order to address the various disadvantages of the optimal energy management systems proposed in the literature, we present in this work a novel solution of an optimal control of both active and reactive power flow for isolated microgrids based on fuzzy logic techniques. The performance of this solution that allows a better sharing of the active and reactive power flow will be presented. The stability and reliability of remote microgrids are demonstrated in this work. Active/reactive power control responds quickly to voltage/frequency variations on the AC-link system.

The rest of this paper is structured as follows: The dynamic microgrid model is presented in Section 2. The power management system based on fuzzy logic is presented in Section 3. The simulation results and discussion are presented in Section 4. Lastly, Section 5 presents the conclusions.

2. Dynamic microgrid model

2.1 PV panel model

A photovoltaic cell is basically a semiconductor diode whose p–n junction is exposed to light. Photovoltaic cells are made of several types of semiconductors using different manufacturing processes. The monocrystalline and polycrystalline silicon cells are only found at the commercial scale at the present time [21]. The basic equation from the theoretical operation of semiconductors that mathematically describes the current-voltage (*I-V*) characteristic of the ideal photovoltaic cell is as follows [22]:

Parameters	Value
Maximum power (*Pmax*)	220 W
Voltage at Pmax (*Vmp*)	48.3 V
Current at Pmax (*Imp*)	4.54 A
Open-circuit voltage (*Voc*)	59.26 V
Short-circuit current (*Isc*)	5.09 A
Rs	0.243 Ω
Rp	235.76 Ω

Table 1.
Electrical characteristic data from NREL system advisor model taken at STC.

$$I = I_{ph} - I\left(e^{\frac{q(V+IR_S)}{AKT}} - 1\right) - \frac{V + IR_S}{R_P} \quad (1)$$

where I_{ph} is the photo-generated current, I_0 is the dark saturation current, I_{Rp} is current flowing in the shunt resistance, R_p is the cell series resistance, A is the diode quality factor, k is the Boltzmann constant at 1.38 10^{-23} J/K, and q is the electron of a charge at 1.6 10^{-19} C.

The solar photovoltaic system used in this study consists of 90 CS5P-220 panels connected in series and parallel with each other. The maximum power point tracking (MPPT) voltage and currents are 48.3 V and 4.54 A, respectively, and generate an output power of 220 W. As the output voltage is relatively low, it is necessary to increase the output voltage of the PV system to the desired value of 500 V by using a boost converter. An MPPT algorithm is used to track the MPP to control the boost converter with an appropriate duty cycle to achieve a desired continuous output voltage. The Perturb & Observe (P&O) algorithm is used to determine the desired duty cycle of the boost converter so that the MPPT is reached. The resulting power of the modeled PV generator is 19.7 kW with 90 panels, each having a maximum power of 220 W, as described in **Table 1**. Similarly, a 25 kW wind turbine was also used in this study.

2.2 Wind turbine model

A wind turbine based on the use of a Permanent Magnet Synchronous Generator (PMSG) is considered the second distributed energy resource (DER) in the configuration of our microgrid. The output power of the wind turbine [10] is given by the following relation [23]:

$$p_{mec} = \frac{1}{2}\rho\pi R^2 C_p(\lambda,\beta)v^3 \quad (2)$$

where R is the radius of the wind turbine aerodynamic rotor in meters, Ω is the rotational speed of the rotor in rad/s, and v is the wind linear velocity in m/s. ρ is the air density at the turbine in kg/m^3, Cp designates the fraction of power available in the wind that is converted into mechanical power.

Cp has a theoretical maximum value of 0.593 (Betz' limit), and basically depends on the tip speed ratio λ, and the blade pitch angle, β can be expressed as follows [23]:

$$C_p(\lambda,\beta) = 0.5\left(\frac{116}{\lambda_i} - 0.4\beta - 5\right)e^{-\frac{21}{\lambda_i}} \tag{3}$$

with

$$\lambda_i = \left(\frac{1}{\lambda + 0.08\beta} - \frac{0.035}{\beta^3 + 1}\right)^{-1} \tag{4}$$

Generally, wind turbines are characterized by two parameters: tip speed ratio (λ) and power coefficient (Cp). The tip speed ratio is defined as:

$$\lambda = \frac{R\Omega}{v} \tag{5}$$

Figure 1 illustrates the characteristic curves of the power coefficient obtained from (Eq. (4)). In order for the wind turbine to extract the maximum available wind power at a given wind speed, the operating point of the turbine must be kept in the λ_{opt} area. Consequently, a Maximum Power Point Tracking (MPPT) algorithm, which is detailed below, is needed to control the rotational rotor velocity of the turbine and maintain it at the maximum power.

In order to achieve the PMSG control system, its dynamic model is required. The generator model is derived from the projection of its equations on a reference coordinate system rotating synchronously with the magnet flux. In order to achieve synchronization between the dq rotating reference frame and the abc three-phase frame, a phase-locked loop (PLL) is used. Then, a dynamic model of the surface mounted PMSG is expressed as:

$$\begin{cases} v_{ds} = R_s i_{ds} + L_s \dfrac{di_{ds}}{dt} - \omega\psi_{qs} \\ v_{qs} = R_s i_{qs} + L_s \dfrac{di_{qs}}{dt} + \omega\psi_{ds} \end{cases} \tag{6}$$

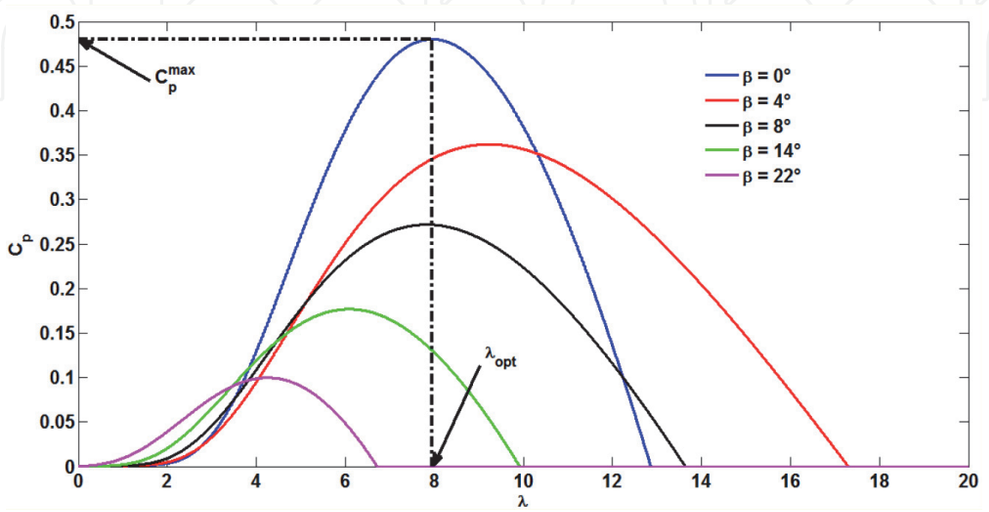


Figure 1.
Power coefficient curves versus tip speed ratio for different blade angles.

where Ls and R_s are the generator inductance and resistance, respectively, ω is the electrical generator speed, and Ψ_{ds} and Ψ_{qs} are d-axis and q-axis magnet flux, respectively, which are expressed as follows:

$$\begin{cases} \psi_{ds} = L_s i_{ds} + \varphi \\ \psi_{qs} = L_s i_{qs} \end{cases} \tag{7}$$

where Φ is the magnet flux. Then, the electrical model of PMSG in the synchronous reference frame can be expressed as:

$$\begin{cases} \dfrac{di_{ds}}{dt} = \dfrac{1}{L_s}\left(-R_s i_{ds} + \omega L_s i_{qs} + v_{ds}\right) \\ \dfrac{di_{qs}}{dt} = \dfrac{1}{L_s}\left(-R_s i_{qs} - \omega L_s i_{ds} - \omega \varphi + v_{qs}\right) \end{cases} \tag{8}$$

The electromagnetic torque of the non-salient poles PMSG is written as:

$$T_{em} = \frac{3}{2} p \ \ \varphi i_{qs} \tag{9}$$

where p is the number of pole pairs of the generator. Eq. (9) shows that the generator torque can be controlled directly via the q-axis current of the stator.

The mechanical dynamics model of the considered wind turbine system can be defined by the following expression:

$$J_T \frac{d\omega_r}{dt} + f\,\omega_r = T_T - T_{em} \tag{10}$$

where T_T represents the mechanical torque, J_T is the moment of inertia, F is the coefficient of friction, and ω_r is the mechanical speed, which is related to the electrical rotation as follows:

$$\omega = p\,\omega_r \tag{11}$$

2.3 Diesel genset model

The diesel generator is composed of the internal combustion engine and Wound Rotor Synchronous Generator (WRSG) [23].

2.3.1 Diesel motor model

The diesel engine model is shown in **Figure 2** [24–26]. The dynamic of the actuator is modeled by a first order model with time constant τ_1 and gain K_1 [24, 27]. The combustion block is represented with gain K_2 and delay τ_2 [26].

The actuator is modeled as follows [23]:

$$\frac{K_1}{1 + s\tau_1} \tag{12}$$

The combustion block can be expressed as follows:

$$K_2 e^{s\tau_2} \tag{13}$$

As for the delay, it can be modeled as follows:

$$\tau_2 = \frac{60h}{2Nn_c} + \frac{60}{4N} \tag{14}$$

where h represents the number of strokes, n_c is the number of cylinders, N is the speed of the diesel generator (rpm), and Φ is the fuel consumption rate (kg/s) [28]. In order to maintain the grid frequency (AC-bus) constant, the speed of the diesel engine must be kept constant when the load varies.

2.3.2 Synchronous generator model

The simplified model of the Wound Rotor Synchronous Generator (WRSG) can be obtained in dq frame (conversion between abc and dq can be realized by means of the Park Transform) [29].

The stator armature windings voltages are:

$$\begin{cases} v_d = -R_s i_d + \dfrac{d\lambda_d}{dt} - \omega\lambda_q \\ v_q = -R_s i_q + \dfrac{d\lambda_q}{dt} + \omega\lambda_d \end{cases} \tag{15}$$

where R_s is the stator winding resistance. The stator fluxes are described by the following formula:

$$\begin{cases} \lambda_d = -L_d i_d + L_{md}\left(i_f + i_D\right) \\ \lambda_q = -L_d i_q + L_{mq} i_Q \end{cases} \tag{16}$$

The rotor armature winding voltage of a synchronous generator is described as:

$$v_f = -R_f i_f - L_d \frac{di_d}{dt} + L_f \frac{di_f}{dt} + L_{md} \frac{di_D}{dt} \tag{17}$$

Damper windings are expressed by the following equation:

$$\begin{cases} 0 = R_D i_D - L_{md} \dfrac{di_d}{dt} + L_{md} \dfrac{di_f}{dt} + L_D \dfrac{di_D}{dt} \\ 0 = R_Q i_Q - L_{mq} \dfrac{di_q}{dt} + L_Q \dfrac{di_Q}{dt} \end{cases} \tag{18}$$

The electromagnetic torque of the synchronous generator can be expressed as follows:

$$T_{em} = p\left(\left(L_d - L_q\right) i_d i_q + L_{md} i_f i_q + L_{md} i_q i_D - L_{mq} i_d i_Q\right) \tag{19}$$

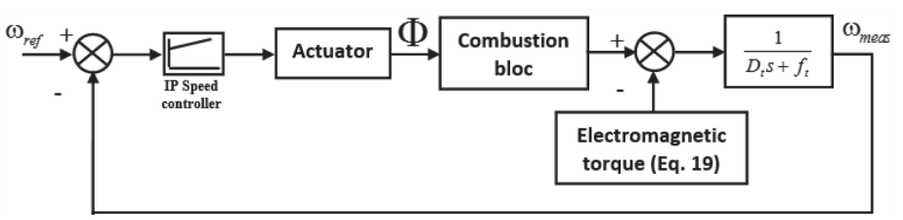


Figure 2.
Block diagram of a diesel generator model [23].

2.4 Electrical load model

In this article, we use a configuration of a dynamic three-phase load as shown in **Figure 3**, which allows us to impose any load profile. As illustrated in **Figure 3**, the gain G is used to transform the active power profile to current ones. Therefore, the three-phase active power can be expressed as follows:

$$P_{load} = \sqrt{3} V_{L-L} I \cos\phi \tag{20}$$

where $V_{L\text{-}L}$ is the line-line voltage of the microgrid. As we are using a three-phase resistor load, relation (20) can be expressed as follows:

$$I = \frac{P_{load}}{\sqrt{3} V_{L-L}} \tag{21}$$

where the gain G is calculated as follows:

$$G = \sqrt{3} V_{L-L} \tag{22}$$

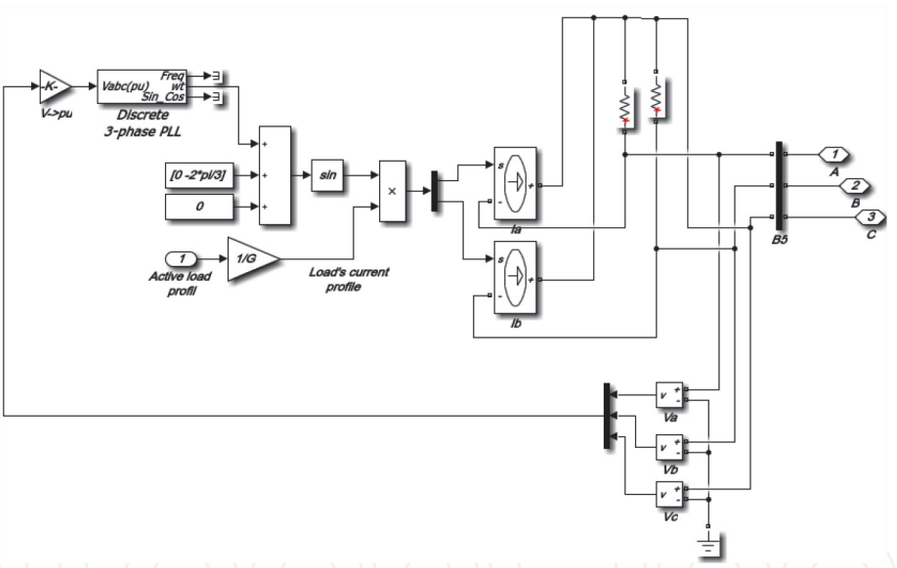


Figure 3.
Matlab block of dynamic three-phase load.

3. Methodology: power management system for remote microgrid based on fuzzy logic

The power management system (PMS) for remote microgrids is presented in this section. Two control levels have been used for the PMS. The second control level is based on the fuzzy logic algorithms, which balance the active power between two diesel generators (master and slave) and regulate the reactive power according to the load demand. The first control level is responsible for following the reference control between all components of the microgrid. The artificial intelligence (AI) algorithm maintains the stability of the remote microgrid and the supply of electricity to the load demand. The PMS based on fuzzy logic is normalized with the aim of ensuring its adaptability to different microgrid sizes.

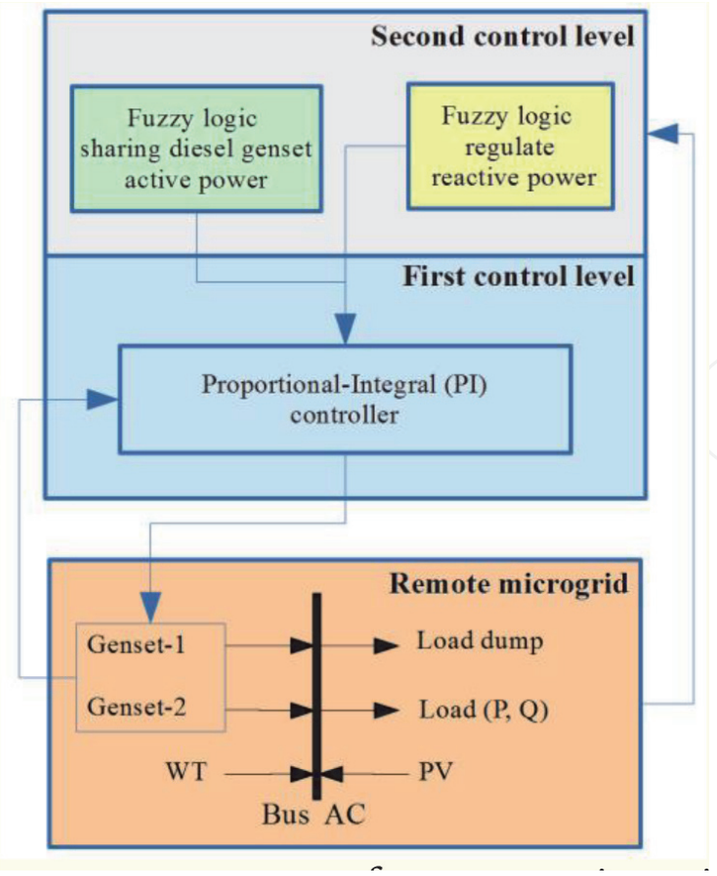


Figure 4.
Power management system for remote microgrid based on artificial intelligence (AI) algorithms.

Figure 4 presents the PMS for remote microgrids based on artificial intelligence (AI) algorithms. The remote microgrid is composed of two diesel generators (genset). The genset-1 (master) is responsible for controlling the frequency/voltage of the microgrid and to maintain its reliability. The genset-2 (slave) is used in operation when the load demand is higher than genset-1 rated power. The remote microgrid is composed of (i) an active/reactive electric load, (ii) a load dump, (iii) PV solar system and (iv) a wind turbine (WT). In this study, the energy storage system (ESS) has not been taken into consideration.

3.1 Second control level

3.1.1 Fuzzy logic controller overview: sharing diesel genset active power

An overview of the architecture of the fuzzy logic controller is presented in **Figure 5**. The fuzzy logic control system aims to balance active power between demand and generation in the remote microgrid for maintaining system reliability. Thus, the gensets (1 and 2) can run simultaneously; two outputs of fuzzy logic controllers are necessary. Pg1* and Pg2* are therefore designed as the output variables of the fuzzy logic system or set points. The centroid method is used for defuzzication.

In order to maintain the efficiency of the fuzzy control systems in terms of rules and decisions, we consider different linguistic variables. Therefore ΔP used 18 linguistic variables as shown in **Figure 6(a)**. Lastly, Pg1* and Pg2* are respectively depicted with 9 and 11 linguistic variables each, as represented in **Figure 6(b)** and **(c)**.

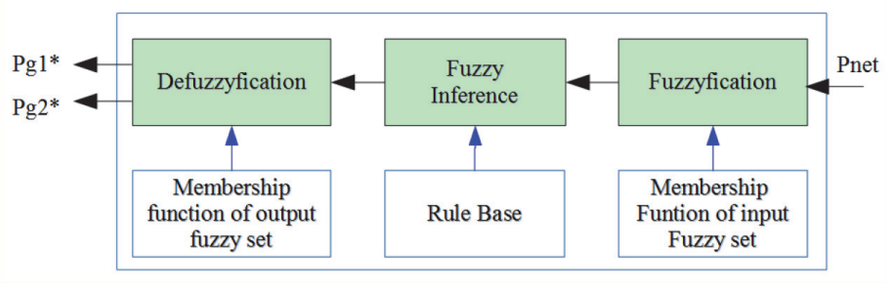


Figure 5.
Fuzzy inference system – sharing diesel genset active power.

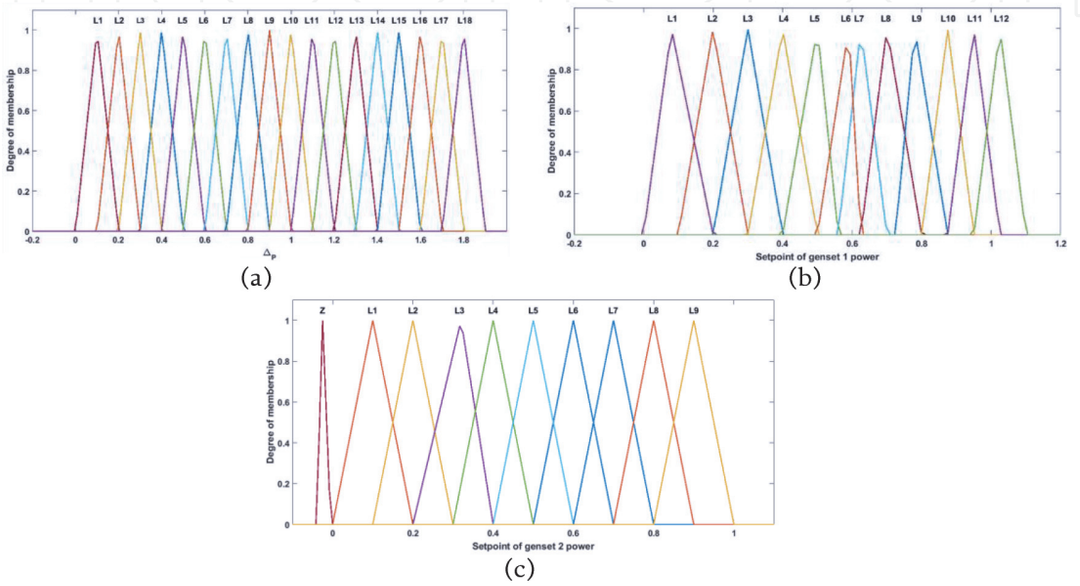


Figure 6.
FL-membership function balance active power: (a) balancing active power between demand and generation in microgrid, (b) set point of genset 1 active power (Pg1) and (c) set point of genset 2 active power Pg2*.*

The trapezoidal and triangular membership functions are used for the linguistic variables' input/output of the fuzzy control system with the aim of simplifying computer calculations on the remote microgrid control (see **Figure 6**).

3.1.2 Fuzzy logic controller overview: regulate reactive power

An overview of the architecture of the fuzzy logic controller is presented in **Figure 7**. The fuzzy logic control system aims to regulate the reactive power in

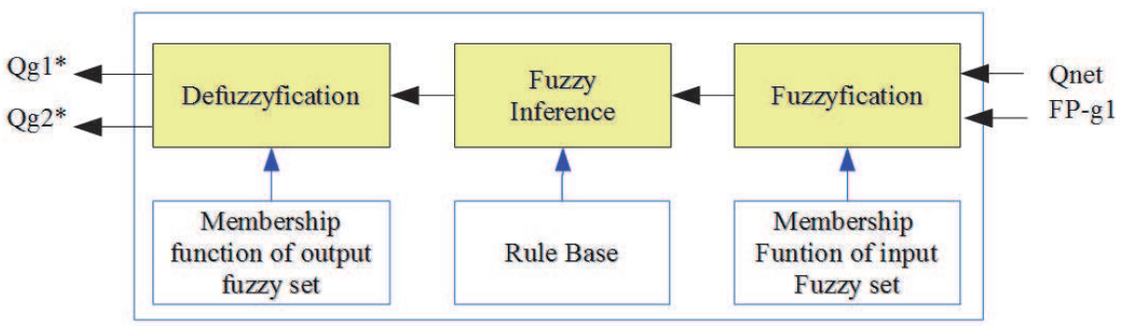


Figure 7.
Fuzzy inference system – regulate reactive power.

remote microgrids in order to maintain their reliability. Thus, regulation of reactive power across the remote microgrid can be performed simultaneously on the two-genset system; two outputs of fuzzy logic controllers are necessary. Thus, Qg1* and Qg2* are designed as the output variables of the fuzzy logic system or setpoints. The centroid method is used for defuzzication.

In order to maintain the efficiency of the fuzzy control systems in terms of rules and decisions, we consider different linguistic variables. Therefore, ΔQ used 16 linguistic variables as shown in **Figure 8(a)**. The measurement of the active power of Genset 2 used two linguistic variables each as represented in **Figure 8(b)**. The set points of Genset 1 and Genset 2 are depicted with six linguistic variables each, as represented in **Figure 8(c)** and **(d)**. Lastly, the FIS output surface of reactive power of Genset 1 is presented in **Figure 8(e)**.

The trapezoidal and triangular membership functions are used for the linguistic variables' input/output of the fuzzy control system with the aim of simplifying computer calculations on the remote microgrid control (see **Figure 8**).

3.2 First control level

The first control level is responsible for following the reference control signal for all distributed energy resources (DER). A proportional integral controller (PI) is used for controlling both the frequency and voltage of the microgrid through the

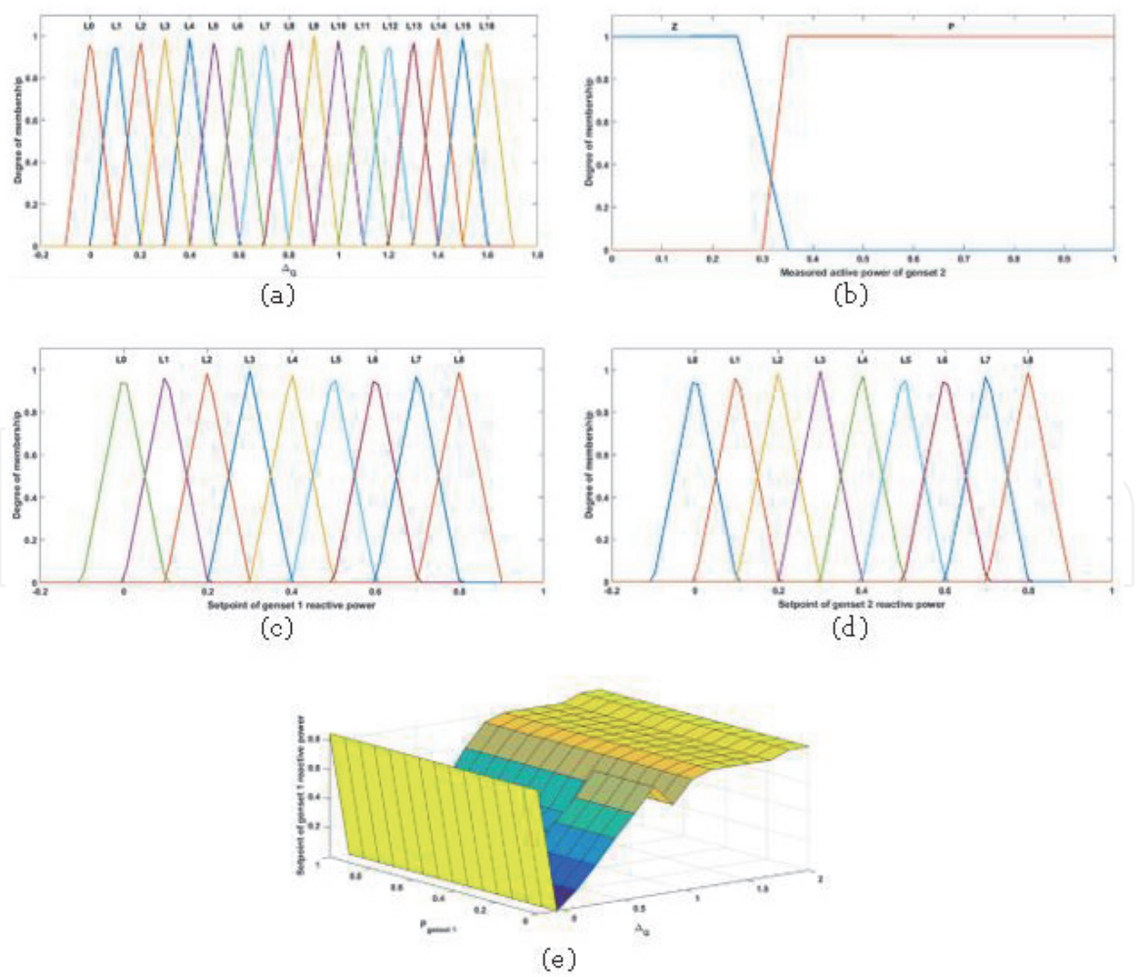


Figure 8.
FL-membership functions regulate reactive power: (a) balancing reactive power between demand and generation in microgrid, (b) measured active power of Genset 2, (c) setpoint of Genset 1 reactive power, (d) setpoint of Genset 2 reactive power and (e) FIS output surface of reactive power of Genset 1.

diesel generators. The diesel genset speed control (frequency) and the AVR control diesel genset control (voltage) are presented in this section.

Likewise, a PV solar system control using the MPPT algorithm based on the fuzzy logic technique and the PV inverter control is depicted in this section. Additionally, the wind turbine system control based on the MPPT algorithm and the grid side converter (GSC) control is presented in this section. Both MPPT algorithms are based on the perturbation and observation (P&O) technique.

3.2.1 Fuzzy logic controller overview: regulate reactive power

Figure 9 represents the speed control used for the diesel generator. The modeling of the diesel generator governor is presented by Eqs. (12)–(14). Eqs. (15)–(18) present the modeling of the synchronous generator.

Table 2 presents the PI controller parameters and the governor dynamic coefficients.

3.2.2 AVR control diesel genset

Figure 10 represents the Automatic Voltage Regulator (AVR) control diesel genset used for the diesel generator. The modeling of the synchronous generator is presented by Eqs. (15)–(18).

Table 3 presents the PI controller parameters.

3.2.3 PV solar system control

A new control algorithm for the PV system based on fuzzy logic is presented in this section. The P&O technique is used and implemented with the MPPT methodology. The power electronics converter control of the PV system is also presented in this section.

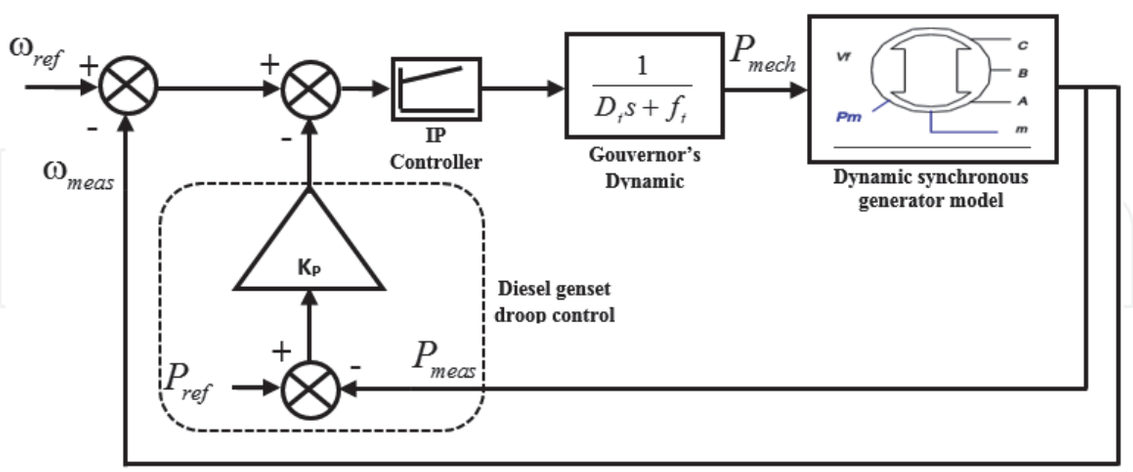


Figure 9.
Diesel genset speed control model.

PI parameters	Governor dynamic coefficients
Kp = 520	0.852
Ki = 240	2–0.15

Table 2.
PI controller parameters and governor dynamic coefficients.

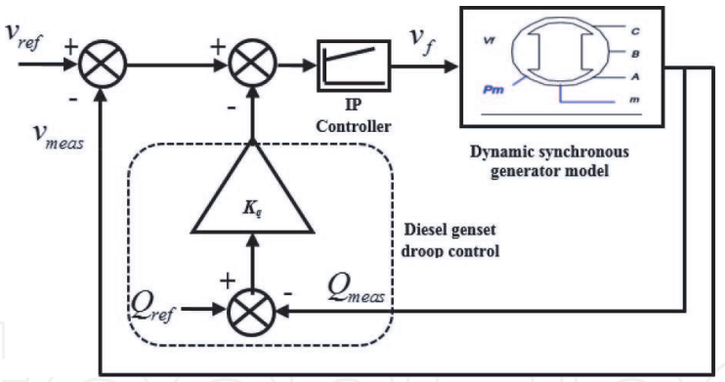


Figure 10.
Diesel genset AVR control model.

PI parameters	
Kp	12
Ki	5

Table 3.
AVR PI controller parameters.

3.2.3.1 MPPT algorithm based on fuzzy logic techniques

An overview of the architecture of MPPT algorithms based on fuzzy logic used in PV solar system control is presented in **Figure 11**. The fuzzy logic control system aims to control the PV converter system. The MPPT method is based on the perturbation & observation (P&O) technique. The maximum PV active power is extracted to every moment with the P&O technique. The variation of active power (Δp) and the variation of DC voltage (Δv) of PV systems are the inputs to the MPPT system. The duty cycle to control the dc-dc boost converter corresponds to the output of the MPPT system. The fuzzy logic used the centroid method for defuzzication.

In order to maintain the efficiency of the fuzzy control systems in terms of rules and decisions, we consider different linguistic variables. Therefore, Δp and Δv used five linguistic variables as shown in **Figure 12(a)** and **(b)**. The duty cycle used five linguistic variables each, as represented in **Figure 12(c)**. **Table 4** presents the names of the linguistic variables.

The trapezoidal and triangular membership functions are used for the linguistic variables' input/output of the fuzzy control system with the aim of simplifying computer calculations (see **Figure 12**).

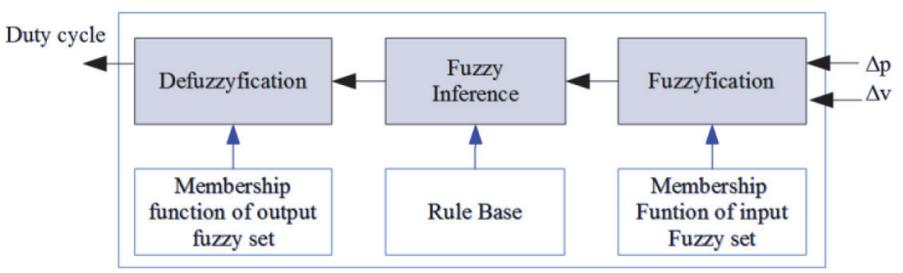


Figure 11.
Fuzzy inference system – MPPT algorithm for PV control.

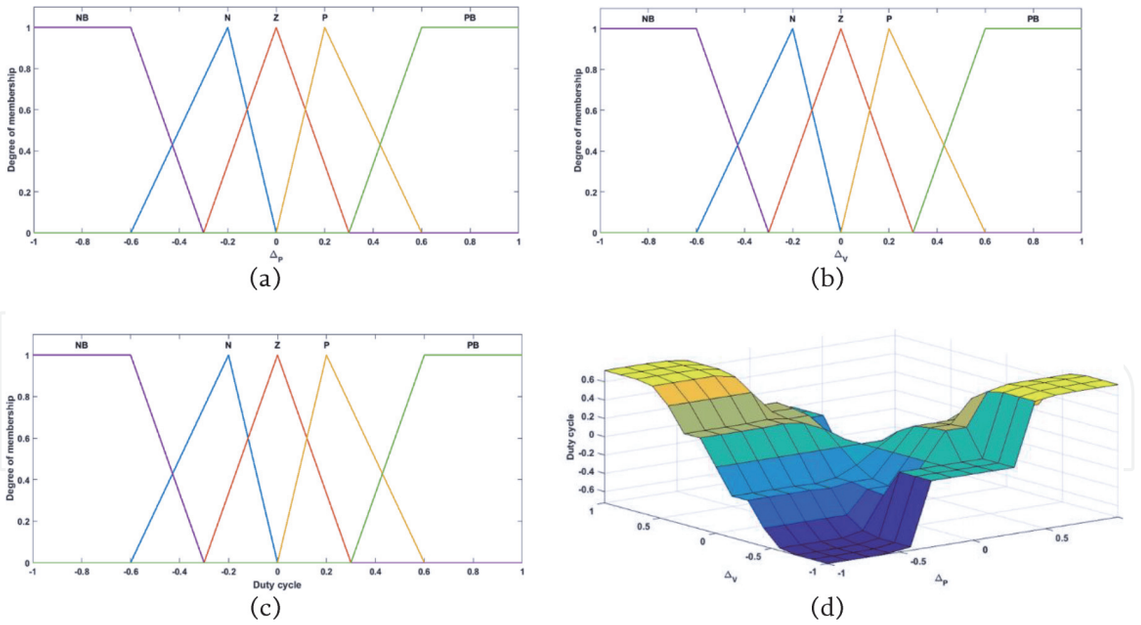


Figure 12.
FL-membership function MPPT algorithm for PV system: (a) variation of active power, (b) variation of DC voltage, (c) boost converter duty cycle and (d) FIS output surface of MPPT algorithms.

Linguistic variable	Description
NB	Negative big
N	Negative
Z	Zero
P	Positive
PB	Positive, big

Table 4.
Linguistic variables.

3.2.3.2 PV solar inverter control

The three-phase two-sage photovoltaic grid-connected system used with its overall control is illustrated in **Figure 13**. The system contains three controllers. A two-loop controller controls the three-phase PV inverter. The outer loop controls both the dc-link voltage to follow the reference value (Vdc_{ref}) and reactive power and to provide the values (Idq_{ref}) of the reference current (i_{ref}) for the inner loop. A phase-locked loop (PLL) algorithm is used to obtain this signal. The current control loop controls the inverter current (i_d and i_q) according to the reference current (i_{ref}). An MPPT algorithm is used to track the maximum power from the PV array regardless of the variation of both solar irradiance and temperature.

3.2.4 Wind turbine system control

3.2.4.1 MPPT algorithm

An overview of the architecture of MPPT algorithms for the WT system based on fuzzy logic is presented in **Figure 14**. The objective of the fuzzy logic control

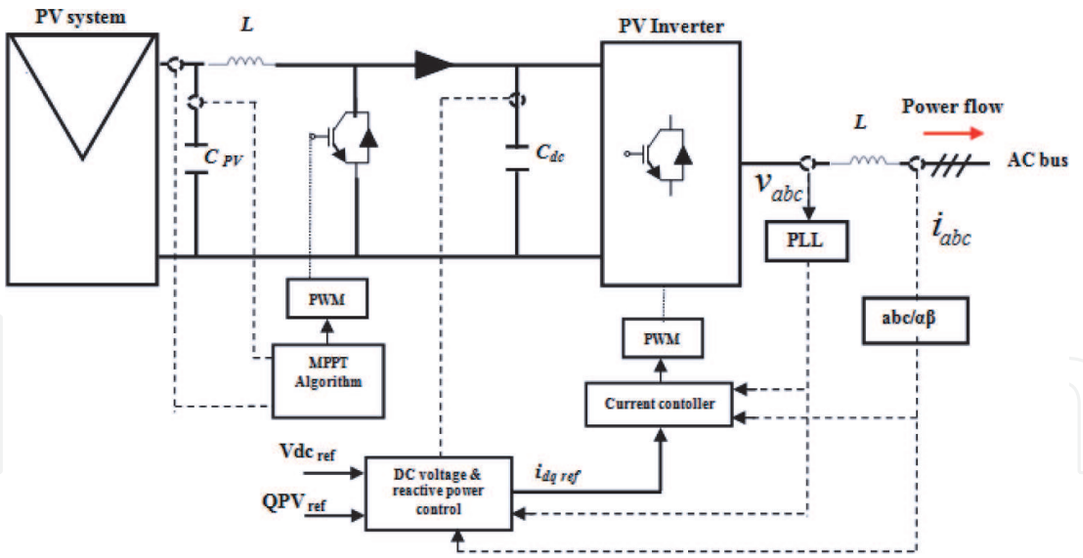


Figure 13.
Proposed three-phase, two-stage grid-connected PV system.

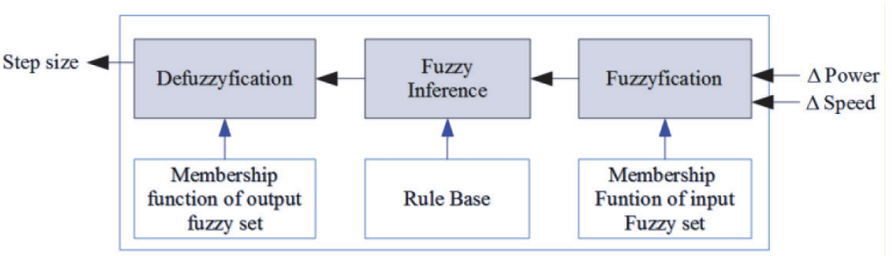


Figure 14.
Proposed wind turbine MPPT algorithm.

system is the calculation of the set point of the generator to track the maximum power point regarding the wind speed variation. The instantaneous generated wind power and its variation represent the respective inputs of the MPPT system. The setpoint of the generator is the output of the used FL MPPT algorithm.

In order to extract the maximum wind power, we have applied in this article the fuzzy logic. Thus, the set point of the speed of the generator is constantly calculated in order to follow the maximum power as a function of the variation of the wind speed. In order to avoid disturbances, the variation step of the generator speed setpoint is proportional to the difference between the maximum power and the real power. The name of the linguistic variables used is the same as represented in **Table 4**.

The control strategy of the fuzzy logic is based on an expert human operator to interpret a situation and initiate its appropriate command action [30]. Commonly, a controller based on fuzzy logic has two inputs and provides a control action. For FLC P&O, inputs are quantized into 5 levels represented by a set of linguistic variables: Negative Big (NB), Negative (N), Zero (Z), Positive (P), and Positive Big (PB). The fuzzy rule base formulation of FLCP&O is shown in **Table 5**. These rules are chosen to perform the optimization of wind generation capture as follows: (i) when the input signals are far from the optimal point, the output of the FLCP&O provides a big step size; (ii) when the inputs are close to the optimum point, the output is set to a small step size value; (iii) once the inputs are close to the optimum point, the step size is set to zero. In this article, we use the min and max operators as

Step size		ΔPower				
		NB	**N**	**Z**	**P**	**PB**
ΔSpeed	NB	NB	N	Z	P	PB
	N	NB	N	Z	P	PB
	Z	NB	N	Z	P	PB
	P	NB	N	Z	P	PB
	PB	NB	N	Z	P	PB

Table 5.
Membership functions of output variables [31].

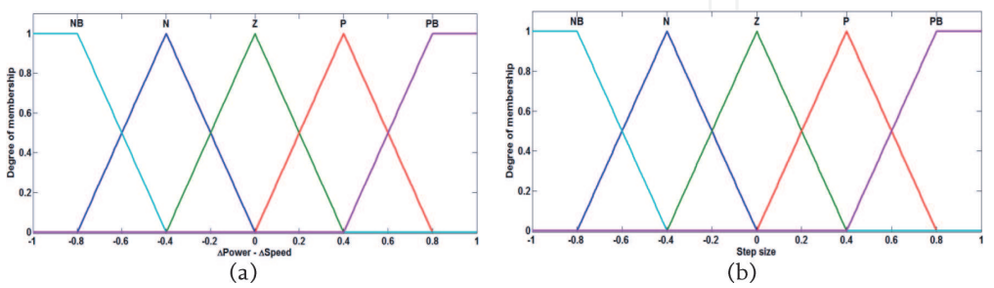


Figure 15.
FL-membership function MPPT algorithms for WT control: (a) membership functions of inputs variables and (b) membership functions of output variables.

t-norm and t-conorm, respectively. Triangular membership functions are used, principally due to their efficiency and high-performance computing. The membership adopted for both input and output variables are illustrated in **Figure 15(a)** and **(b)**, respectively [31].

3.2.4.2 Rotor side converter (RSC) and grid side converter (GSC)

Figure 16 presents the control system of a wind turbine (WT) system that uses a permanent magnet synchronous generator (PMSG). The MPPT method extracts the maximum power from the WT using the P&O technique. The MPPT output signal control or duty cycle is sent to the rotor side converter (RSC).

Figure 17 presents in detail the application of the MPPT algorithm for controlling the wind turbine. The WT rotation is measured (Ωmes) on the WT shaft. The reference value of the WT shaft rotation (Ω_{ref}) is determined by MPPT fuzzy logic.

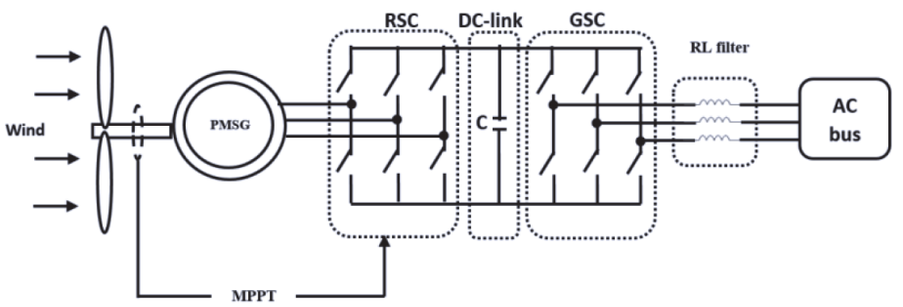


Figure 16.
Block diagram of direct-drive wind turbine system.

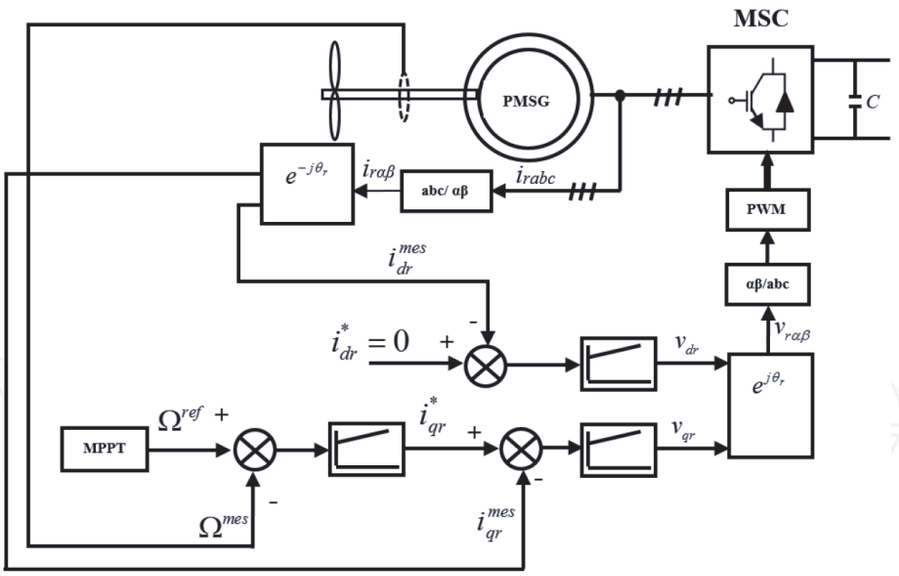


Figure 17.
MPPT control scheme for wind turbine system.

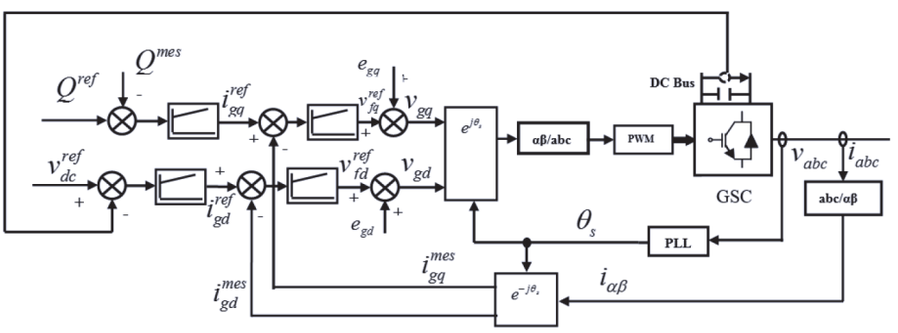


Figure 18.
GSC control scheme for wind turbine system.

The objective of the grid-side converter is to keep the DC-link voltage fixed and adjust the absorbed or provided reactive power according to grid code requirements. As shown in **Figure 18**, the active and reactive power can simply be controlled by d-axis and q-axis current using the grid voltage-oriented control. This control strategy contains two nested loops. The inner loop controls the grid current while the outer loop regulates the DC-link voltage and reactive power for the GSC. The DC-link voltage is controlled by d-axis current since it depends on the active power. On the other hand, the q-axis reference is set to zero when a unity power factor is required; otherwise, it is adjusted as a function of the reactive power needed.

4. Simulation and analysis results

The simulation results are presented below. Three simulation scenarios are proposed. The first scenario presents the results of the first control level and second control level of a remote microgrid system with wind speed and solar irradiation stepped profile. The second scenario presents the results of the remote microgrid control using a wind speed and solar irradiation fluctuating profile. Lastly, the third scenario presents the performance evaluation of MPPT-P&O based on fuzzy logic techniques.

4.1 Scenario 1: wind and solar irradiation stepped profile

4.1.1 First control level of remote microgrid

Figure 19 presents the results concerning the first control level of remote microgrids for both controllable and non-controllable energy sources such as diesel generators and renewable energy sources (WT, PV). The solar irradiance and wind speed profiles are presented in **Figure 19(a)** and **(b)**, respectively. The PV system power and the wind turbine active power are shown in **Figure 19(c)** and **(d)**. **Figure 19(e)** and **(f)** present the active power and reactive power load. Lastly, Genset 1

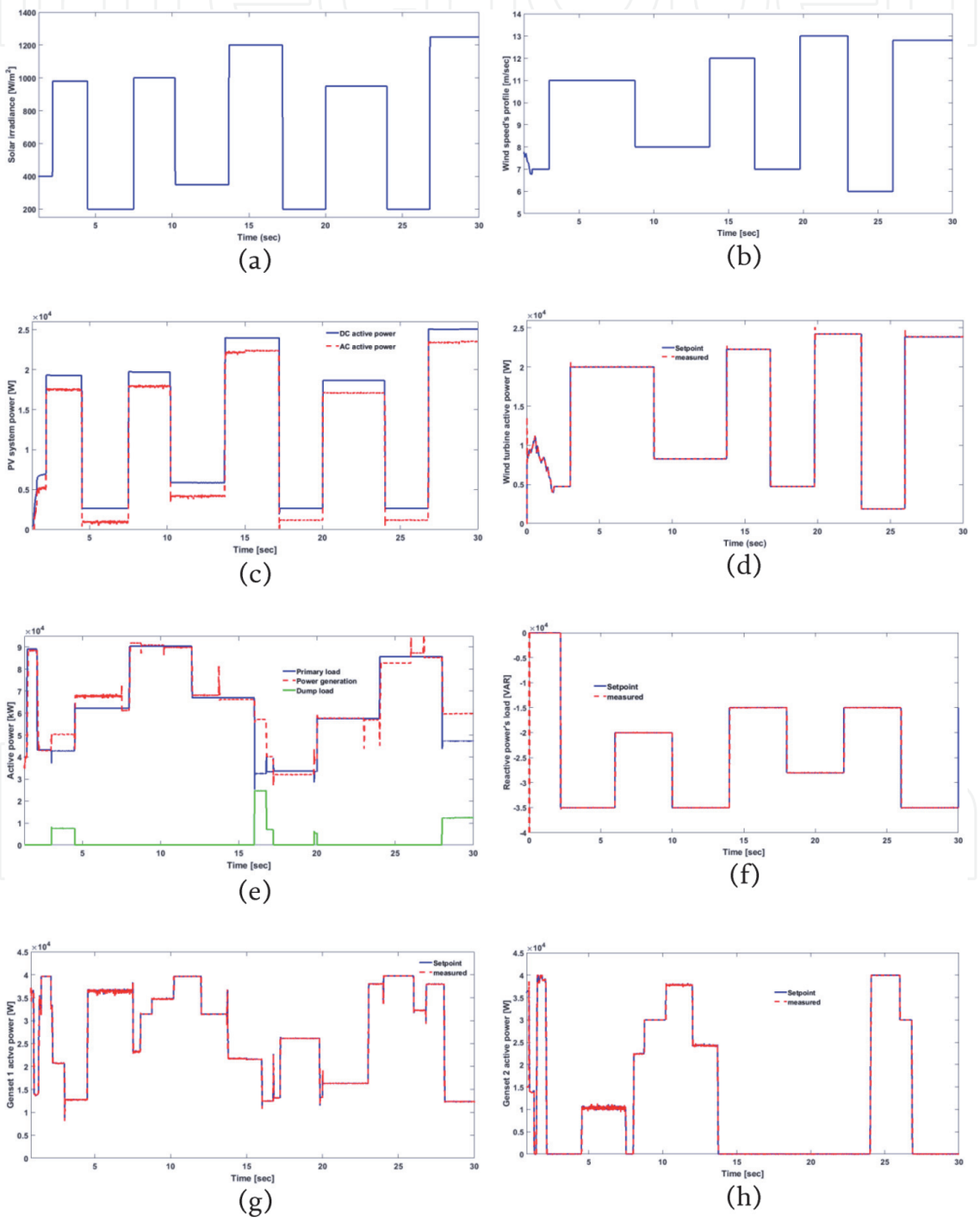


Figure 19.
First control level of remote microgrid results for wind speed and solar irradiation stepped profiles: (a) solar irradiation profile, (b) wind speed profile, (c) PV system power, (d) wind turbine active power, (e) active power, (f) reactive power load, (g) Genset 1 active power and (h) Genset 2 active power.

active power and Genset 2 active power are presented in **Figure 19(g)** and **(h)**, respectively.

4.1.2 Second control level of remote microgrid

Figure 20 presents the results concerning the second level microgrid control for both the controllable and non-controllable energy sources such as diesel generators and renewable energy sources such as PV panels. The sharing of active/reactive power is presented in **Figure 20(a)** and **(b)**, respectively. **Figure 20(c)** presents the microgrid frequency. Lastly, the DC-link voltage of the PV system is shown in **Figure 20(d)**.

4.2 Scenario 2: wind and solar irradiation continuous profile

4.2.1 First control level of remote microgrid

Figure 21 presents the results concerning the first control level of remote microgrids for both controllable and non-controllable energy sources such as diesel generators and renewable energy sources (WT, PV). The solar irradiance and wind speed profiles are presented in **Figure 21(a)** and **(b)**, respectively. The PV system power and the wind turbine active power are shown in **Figure 21(c)** and **(d)**. **Figure 21(e)** and **(f)** presents the active power with dump load and the reactive power load. Lastly, Genset 1 active power and Genset 2 active power are presented in **Figure 21(g)** and **(h)**, respectively.

4.2.2 Second control level of remote microgrid

Figure 22 presents the results concerning the second control level of remote microgrid for both controllable and non-controllable energy sources such as diesel generators and renewable energy sources such as PV panels. The sharing of active/reactive power is presented in **Figure 22(a)** and **(b)** respectively. **Figure 22(c)**

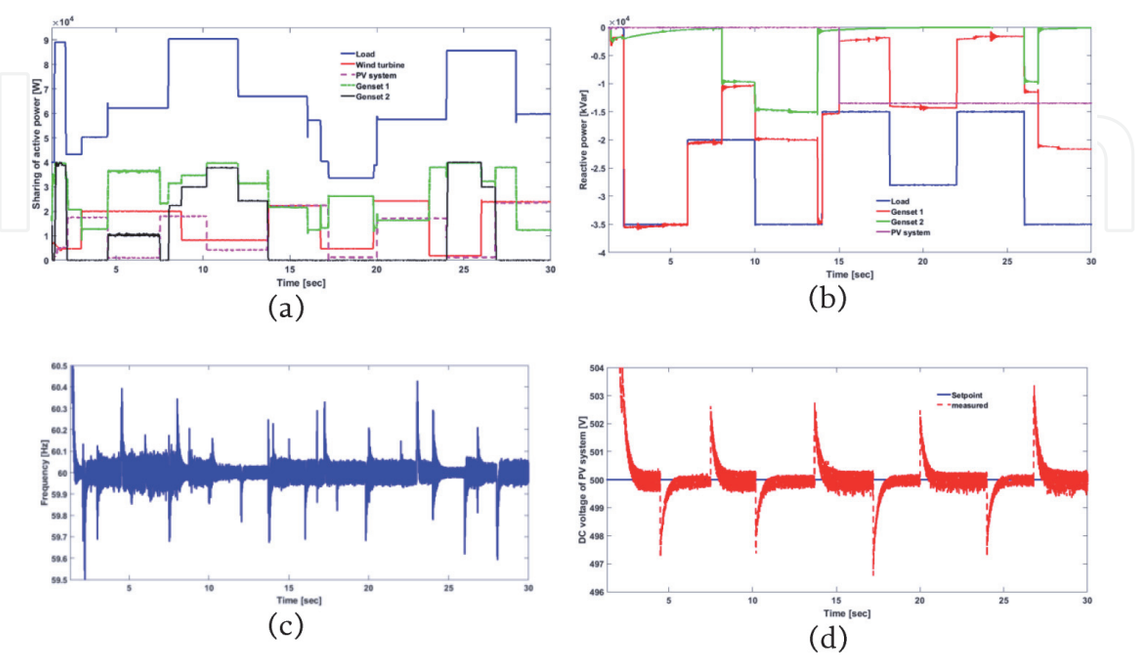


Figure 20.
Second control level remote microgrid results using fuzzy logic techniques: (a) active power sharing, (b) reactive power sharing, (c) microgrid frequency and (d) DC-link voltage of PV system.

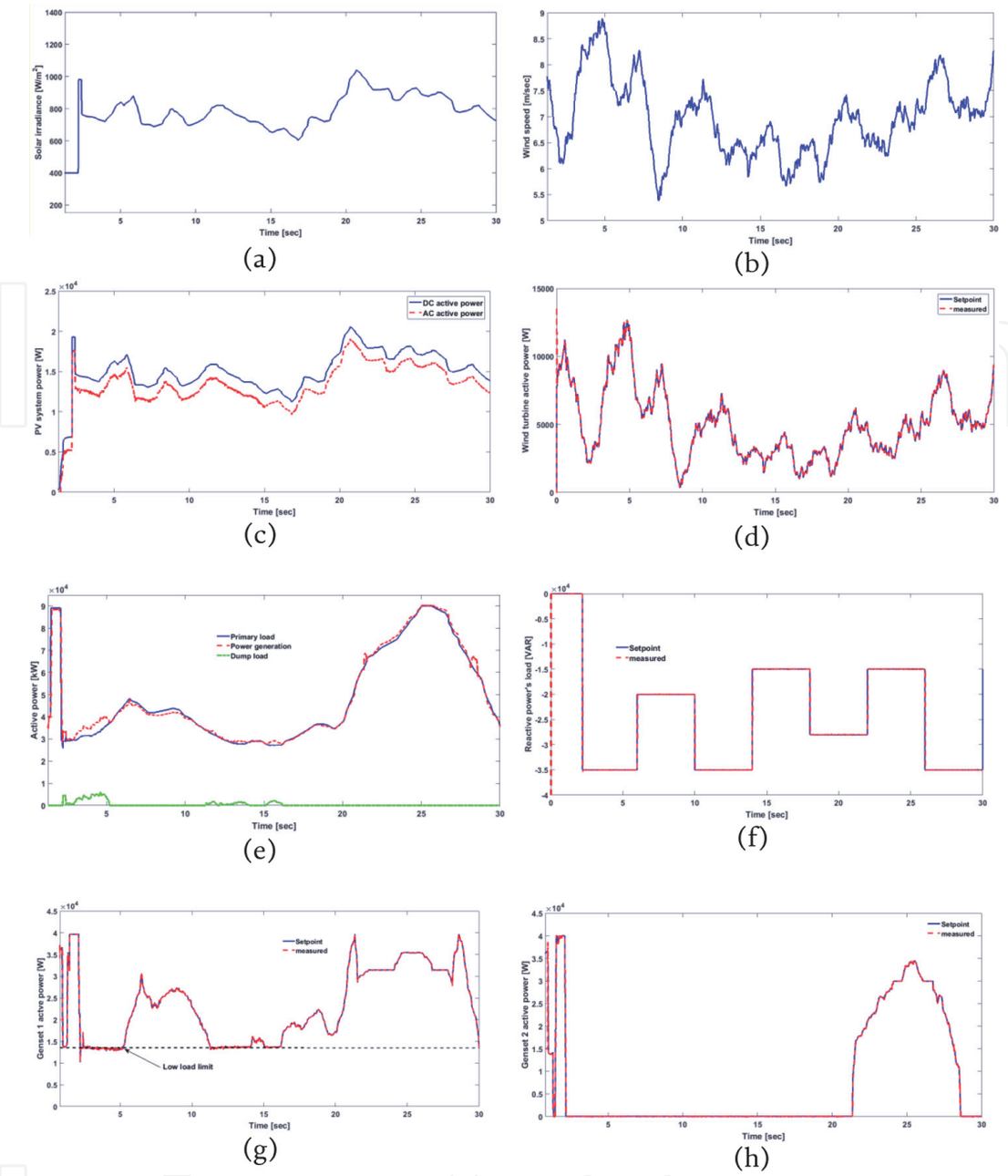


Figure 21.
First control level remote microgrid results for wind speed and solar irradiation stepped profile: (a) solar irradiation profile, (b) wind speed profile, (c) PV system power, (d) wind turbine active power, (e) active power with dump load, (f) reactive power load, (g) Genset 1 active power and (h) Genset 2 active power.

presents the microgrid frequency. Lastly, the DC-link voltage of the PV system is shown in **Figure 22(d)**.

4.3 Scenario 3: performance evaluation of PV systems control: fixed-step P&O, variable-step P&O (MPPT-FL) and inductance method

Several MPPT techniques have been proposed in the literature such as the perturbation and observation (P&O) technique, incremental conductance technique, ripple correlation technique, short-circuit current technique, and open-circuit voltage technique (OCV). These techniques vary in terms of complexity, cost, speed of convergence, required sensors, hardware implementation and efficiency [32–36].

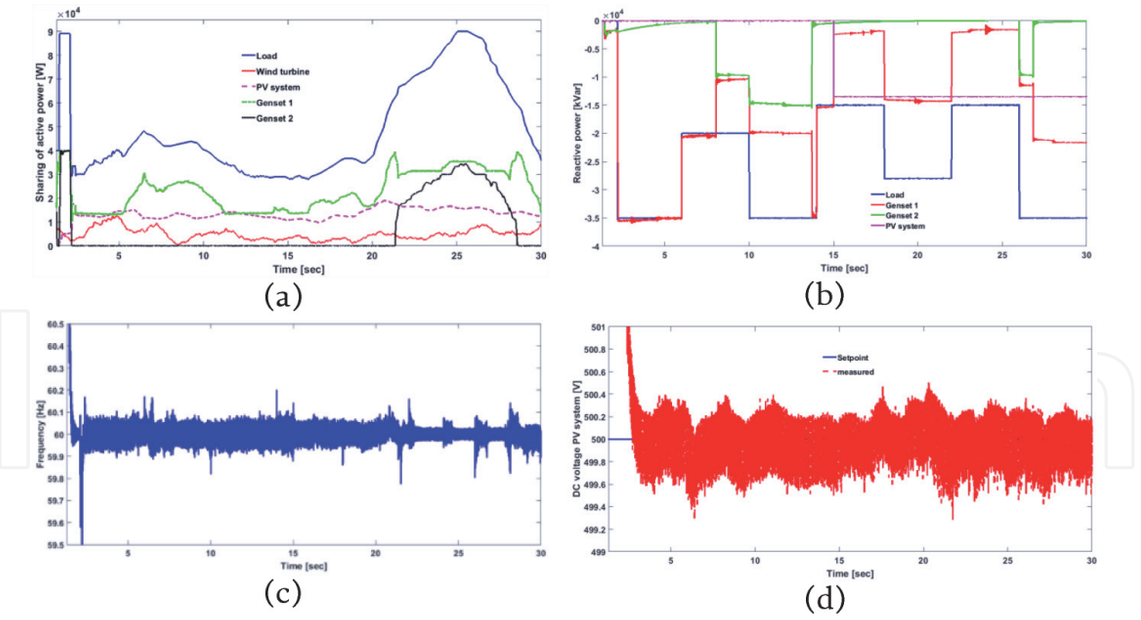


Figure 22.
Second control level remote microgrid results using fuzzy logic techniques: (a) active power sharing, (b) reactive power sharing, (c) microgrid frequency and (d) DC-link voltage of PV system.

Due to the existence of numerous MPPT methods, various researches have presented a comparative analysis of their performance. In fact, some articles present a comparative study of just a few methods while others present a comparison of multiple MPPT methods, based on simulations and from the standpoint of energy production. The MPPT techniques are evaluated while taking into account both solar irradiation and temperature variation and calculation of the total energy provided by the PV solar system.

In this work, we will focus on the simulation of two MPPT techniques (perturbation and observation, and incremental conductance) and compare their performance regarding the proposed MPPT algorithm based on the fuzzy logic techniques presented above. Both P&O and incremental conductance techniques used in this paper are widely presented in the literature [36]. It should be noted that the most significant feature among all MPPT techniques is convergence speed. Thus, any improvement in convergence speed can increase the reliability and robustness of the entire PV system. For this reason, we propose in this work to use a variable step based on fuzzy logic techniques.

In order to achieve good characterization of the different MPPT techniques, simulations were carried out using a Matlab/Simulink environment. The PV solar system was simulated under different operating conditions, especially during transient state caused by a wide variation of the solar radiation.

Table 6 illustrates both efficiency and Total Harmonic Distortion (THD) of each MPPT technique. Note that efficiency was calculated by taking into account the maximum theoretical power and the instantaneous provided power as follows [36]:

$$\eta = \frac{P_{provied}}{P_{\max}} \tag{23}$$

As can be seen in **Table 6**, all tested MPPT techniques have an acceptable THD (less than 5% regarding CEI 61727 standard) at 1000 and 800 W/m^2. However, when solar irradiation fluctuated between 600 and 400 W/m^2 the FL-P&O technique has a better THD than the other two MPPT techniques. For efficiency,

MPPT technique	Efficiency [%]				THD [%]			
	400 W/m^2	600 W/m^2	800 W/m^2	1000 W/m^2	400 W/m^2	600 W/m^2	800 W/m^2	1000 W/m^2
FL P&O	88.26	94.74	97.96	98.46	9.89	5.30	3.93	3.32
Conventional P&O	87.29	94.08	97.61	98.21	12.28	5.80	4.08	3.40
Incremental conductance	87.59	92.75	96.26	97.38	10.46	5.90	3.91	3.71

Table 6.
Performance of different MPPT techniques.

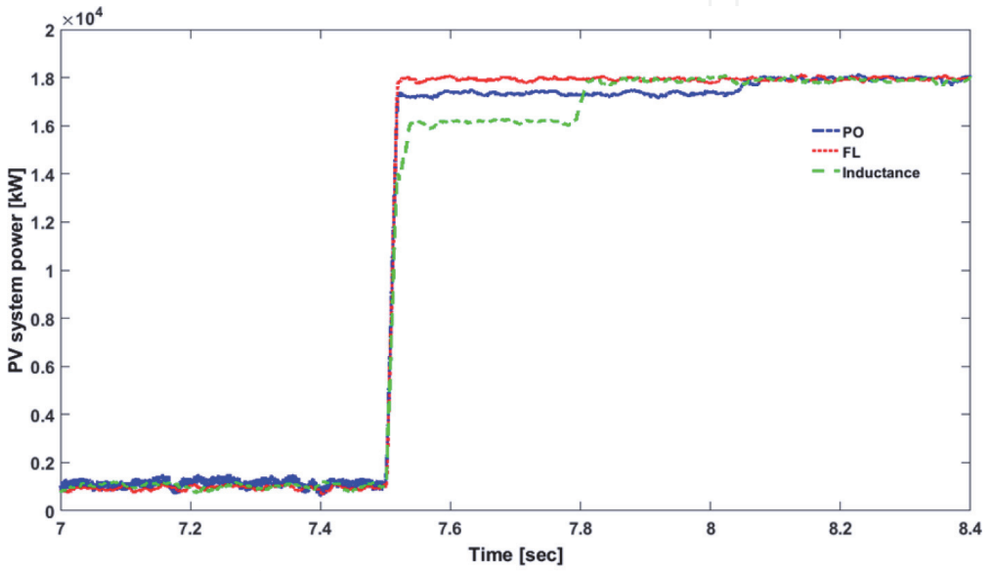


Figure 23.
Performance comparison of three PV MPPT algorithms.

notwithstanding the solar irradiance fluctuation, the FL P&O MPPT has better performance compared to P&O and inductance conductance techniques.

As shown in **Figure 23**, FL-P&O technique has the highest rise time compared to both P&O and incremental conductance techniques. In the steady state, the P&O technique has the slowest convergence speed compared to the other two MPPT techniques.

5. Conclusion

This article presented a novel power flow management algorithm for a remote microgrid based on fuzzy logic. The objectives of this power management system are improved microgrid reliability, improved renewable energy source (RES) integration and performance of active/reactive power control for remote microgrids using artificial intelligence (AI) algorithms.

Sharing of the diesel genset's active and reactive power has been based on AI algorithms such as fuzzy logic. Two simulation scenarios are proposed. The first scenario was used on a wind speed and solar irradiation stepped profile and the second scenario was used on a wind speed and solar irradiation continuous profile.

The results of both scenarios are satisfactory. The stability and reliability of the remote microgrid are demonstrated in the simulation. The active/reactive power control algorithm responds quickly to different events on the remote microgrid, especially to the voltage/frequency variations on the AC-link system. Lastly, improvement to RES integration is demonstrated with the use of a new MPPT algorithm for the PV control system. This MPPT algorithm is based on the P&O method and used fuzzy logic techniques. The simulation results demonstrate the easy adaptability, fast response and efficiency of PV control systems.

Acknowledgements

The authors would like to thank the Natural Sciences and Engineering Research Council (NSERC) for its invaluable support in making this work possible.

Author details

Karim Belmokhtar* and Mauricio Higuita Cano
Nergica, Gaspe, Quebec, Canada

*Address all correspondence to: kbelmokhtar@nergica.com

IntechOpen

© 2020 The Author(s). Licensee IntechOpen. Distributed under the terms of the Creative Commons Attribution - NonCommercial 4.0 License (https://creativecommons.org/licenses/by-nc/4.0/), which permits use, distribution and reproduction for non-commercial purposes, provided the original is properly cited. BY–NC

References

[1] Sen S, Ganguly S. Opportunities, barriers and issues with renewable energy development - a discussion. Renewable and Sustainable Energy Reviews. 2016;**69, 2015**:1170-1181

[2] Guney MS, Tepe Y. Classification and assessment of energy storage systems. Renewable and Sustainable Energy Reviews. 2017;**75**:1187-1197

[3] Akinyele DO, Rayudu RK. Review of energy storage technologies for sustainable power networks. Sustainable Energy Technologies and Assessments. 2014;**8**:74-91

[4] Hosseini SE, Wahid MA. Hydrogen production from renewable and sustainable energy resources: Promising green energy carrier for clean development. Renewable and Sustainable Energy Reviews. 2016;**57**:850-866

[5] Roni MS, Chowdhury S, Mamun S, Marufuzzaman M, Lein W, Johnson S. Biomass co-firing technology with policies, challenges, and opportunities: A global review. Renewable and Sustainable Energy Reviews. 2017;**78**:1089-1101

[6] Cano MH, Agbossou K, Kelouwani S, Dubé Y. Experimental evaluation of a power management system for a hybrid renewable energy system with hydrogen production. Renewable Energy. 2017; **113**:1086-1098

[7] Pegueroles-Queralt J, Bianchi FD, Gomis-Bellmunt O. Control of a lithium-ion battery storage system for microgrid applications. Journal of Power Sources. 2014;**272**:531-540

[8] Haddadi A. Modeling, Control, and Stability Analysis of an Islanded Microgrid. McGill [Theses]. McGill University Libraries. 2015

[9] Shuai Z et al. Microgrid stability: Classification and a review. Renewable and Sustainable Energy Reviews. 2016; **58**:167-179

[10] Olatomiwa L, Mekhilef S, Ismail MS, Moghavvemi M. Energy management strategies in hybrid renewable energy systems: A review. Renewable and Sustainable Energy Reviews. 2016;**62**:821-835

[11] Gao Y, Ai Q. Distributed cooperative optimal control architecture for AC microgrid with renewable generation and storage. International Journal of Electrical Power & Energy Systems. 2018;**96**(2017):324-334

[12] Li X, Li Z. Micro-grid resource allocation based on multi-objective optimization in cloud platform, In: 2017 8th IEEE International Conference on Software Engineering and Service Science (ICSESS). Beijing; 2017. pp. 509-512. DOI: 10.1109/ ICSESS.2017.8342966

[13] Chaouachi A, Kamel RM, Andoulsi R, Nagasaka K. Multiobjective intelligent energy management for a microgrid – Aymen Chaouachi - Academia. IEEE Transactions on Industrial Electronics. 2013;**60**(4):1688-1699

[14] Meng L, Sanseverino ER, Luna A, Dragicevic T, Vasquez JC, Guerrero JM. Microgrid supervisory controllers and energy management systems: A literature review. Renewable and Sustainable Energy Reviews. 2016;**60**: 1263-1273

[15] Zahraee SM, Khalaji Assadi M, Saidur R. Application of artificial intelligence methods for hybrid energy system optimization. Renewable and Sustainable Energy Reviews. 2016;**66**: 617-630

[16] Rajesh KS, Dash SS, Rajagopal R, Sridhar R. A review on control of ac microgrid. Renewable and Sustainable Energy Reviews. 2017;**71**:814-819

[17] Gayatri MTL, Parimi AM, Pavan Kumar AV. A review of reactive power compensation techniques in microgrids. Renewable and Sustainable Energy Reviews. 2018;**81**:1030-1036

[18] Kofinas P, Dounis AI, Vouros GA. Fuzzy Q-learning for multi-agent decentralized energy management in microgrids. Applied Energy. 2018;**219**: 53-67

[19] Daoud MI, Abdel-Khalik AS, Elserougi A, Massoud A, Ahmed S, Abbasy NH. An artificial neural network based power control strategy of low-speed induction machine flywheel energy storage system. International Journal of Advanced Information Technology. 2013;**4**(2):61-68

[20] Mallesham G, Mishra S, Jha AN. Automatic generation control of microgrid using artificial intelligence techniques. In: IEEE Power & Energy Society General Meeting. San Diego, CA; 2012. pp. 1-8. DOI: 10.1109/PESGM.2012.6345404

[21] Banu IV, Istrate M. Modeling and simulation of photovoltaic arrays. Buletinul AGIR. 2012;**3**:161-166

[22] Tian H, Mancilla-david F, Ellis K, Jenkins P, Muljadi E. A detailed performance model for photovoltaic systems. United States. Available from: https://www.osti.gov/servlets/purl/1048979

[23] Doumbia ML, Belmokhtar K, Agbossou K. Wind diesel hybrid power system with hydrogen storage. New Developments in Renewable Energy. 2013:365

[24] Roy S, Malik OP, Hope GS. A k-step predictive scheme for speed control of diesel driven power plants. IEEE Transactions on Industry Applications. 1993;**29**(2):389-396

[25] Pena R, Cardenas R, Clare J, Asher G. Control strategy of doubly fed induction generators for a wind diesel energy system. In: IEEE 2002 28th Annu. Conf. Ind. Electron. Soc. IECON 02. Vol. 4. 2002. pp. 3297-3302

[26] Dettmer R. Revolutionary energy a wind/diesel generator with flywheel storage. IEE Review. 19 April 1990;**36** (4):149-151, DOI: 10.1049/ir:19900060

[27] PeÑa R, CÁrdenas R, Proboste J, Clare J, Asher G. Wind-diesel generation using doubly fed induction machines. In: IEEE Transactions on Energy Conversion. Vol. 23. no. 1. March 2008. pp. 202-214. DOI: 10.1109/TEC.2007.914681

[28] Jurado F, Saenz JR. Neuro-fuzzy control for autonomous wind-diesel systems using biomass. Renewable Energy. 2002;**27**(1):39-56

[29] Burton T, Sharpe D, Jenkins N, Bossanyi E. Wind Energy Handbook. Vol. 2. New York: Wiley; 2011

[30] Schneider M, Kandel A, Langholz G, Chew G. Fuzzy expert system tools. Chichester: Wiley; 1996

[31] Belmokhtar K, Ibrahim H, Doumbia ML. A maximum power point tracking control algorithms for a PMSG-based WECS for isolated applications: Critical review. IntechOpen. 2014;**2**: 283-302

[32] Elgendy MA, Zahawi B, Atkinson DJ. Evaluation of perturb and observe MPPT algorithm implementation techniques. In: 6th IET International Conference on Power Electronics, Machines and Drives (PEMD 2012). Vol. 3. 2012. p. 110

[33] Kumar H, Tripathi RK. Simulation of variable incremental conductance method with direct control method using boost converter. In: 2012 Students Conf. Eng. Syst. SCES; 2012. pp. 1-5

[34] Casadei D, Grandi G, Rossi C. Single-phase single-stage photovoltaic

generation system based on a ripple correlation control maximum power point tracking. IEEE Transactions on Energy Conversion. 2006;**21**(2):562-568

[35] Reza Reisi A, Hassan Moradi M, Jamasb S. Classification and comparison of maximum power point tracking techniques for photovoltaic system: A review. Renewable and Sustainable Energy Reviews. 2013;**19**:433-443

[36] Azar Y, DeRubertis B, Baril D, Woo K. Comparison of different MPPT algorithms with a proposed one using a power estimator for grid connected PV systems. Annals of Vascular Surgery. 2017;**43**:44

IntechOpen

IntechOpen